MARIOLA SATERNUS*, JAN BOTOR*

MODELLING OF THE CONTINUOUS REFINING PROCESS OF AK-64 ALLOY

MODELOWANIE PROCESU CIĄGŁEJ RAFINACJI STOPU AK-64

The mathematical description of the hydrogen desorption process from liquid aluminium and its alloys in the bubbling process was presented. The mathematical model based on the equation for the mass transfer coefficient and dimensionless number of the hydrogen concentration introduced by Sigworth and Engh is presented. This mathematical modelling was carried out for the continuous reactor under the atmospheric pressure. Also, the selection of main thermodynamic and kinetic parameters, that are essential to modelling calculations, was done. Among the most important parameters there are: the hydrogen solubility in aluminium and its alloys, the interfacial contact area in the system: liquid metals – the bubble of refining gas (this area can be determined using estimated values of the bubble rise velocity and the bubble diameter), and the mass transfer coefficient. The hydrogen solubility in aluminium alloys can be described basing on the activity coefficient calculated from Wagner's interaction parameters. This model and correctness of assumptions, which were made, were verified. The comparison of the calculated hydrogen concentration with the industrial data for AK-64 alloy refining in a continuous reactor under the atmospheric pressure was carried out. The simulation of the refining process under vacuum based on the experimental data for AK-64 alloy under atmospheric pressure was done.

W pracy przedstawiono matematyczny opis procesu desorpcji wodoru z ciekłego aluminium i jego stopów w procesie barbotażu. Przedstawiono model matematyczny w oparciu o równanie na współczynnik przenikania masy i bezwymiarową liczbę kryterialną Sigwortha i Engha wyrażającą zmianę stężenia usuwanego gazu w czasie. Rozważania modelowe przeprowadzono dla reaktora pracującego w systemie ciągłym w warunkach ciśnienia atmosferycznego. Dokonano selekcji i doboru podstawowych danych fizykochemicznych i parametrów kinetycznych potrzebnych do obliczeń modelowych, w tym: rozpuszczalności wodoru w aluminium w funkcji temperatury; wpływu dodatków stopowych na powyższą rozpuszczalność, opisaną na podstawie zmiany współczynnika aktywności określonego z parametrów oddziaływania Wagnera; pola powierzchni wymiany masy w układzie ciekły metal – pęcherzyk gazu rafinującego, określonej na podstawie oszacowanych wartości szybkości wznoszenia się pęcherzyka gazowego i jego ekwiwalentnej średnicy; współczynnika przenikania masy. Przeprowadzono weryfikację modelu

* WYDZIAŁ INŻYNIERII MATERIAŁOWEJ I METALURGII, POLITECHNIKA ŚLĄSKA, 40-019 KATOWICE, UL. KRASIŃSKIEGO 8

i słuszności przyjętych założeń oraz parametrów, dla wyników uzyskanych w warunkach przemysłowych dla stopu odlewniczego AK-64 rafinowanego w reaktorze ciągłym przy ciśnieniu atmosferycznym. Dokonano również symulacji procesu rafinacji w warunkach próżni na bazie danych doświadczalnych z procesu rafinacji prowadzonej w warunkach ciśnienia atmosferycznego.

1. Introduction

There are many methods of refining from hydrogen in the metallurgical industry, and especially in aluminium production. The increasing demand for higher quality aluminium and lower level of impurities has led to many innovations in aluminium production. Many batch purification processes were replaced by in-line melt treatment in which using chlorine is limited, and it is more popular to mix chlorine with inert gas, especially argon, or even to use only inert gas. The ways the inert gas can be introduced into liquid metal can vary: from the porous plug (469 Alcoa system, DUFI Alusuisse), through the nozzle of special construction (FILD British Aluminium, MINT Consolidated Aluminium), and the various types of rotary impeller (SNIF Union Carbide, 622 Alcoa, Alpur Pechiney, GBF Showa Aluminium, RDU Foseco and AFD Alcan). The analysis of available refining methods and types of refining reactors [1] shows that the most popular are refining reactors with impellers which can generate small gas bubbles ranging from 0,005 m to 0,015 m. A rotary impeller causes also the metal bath to be stirred well.
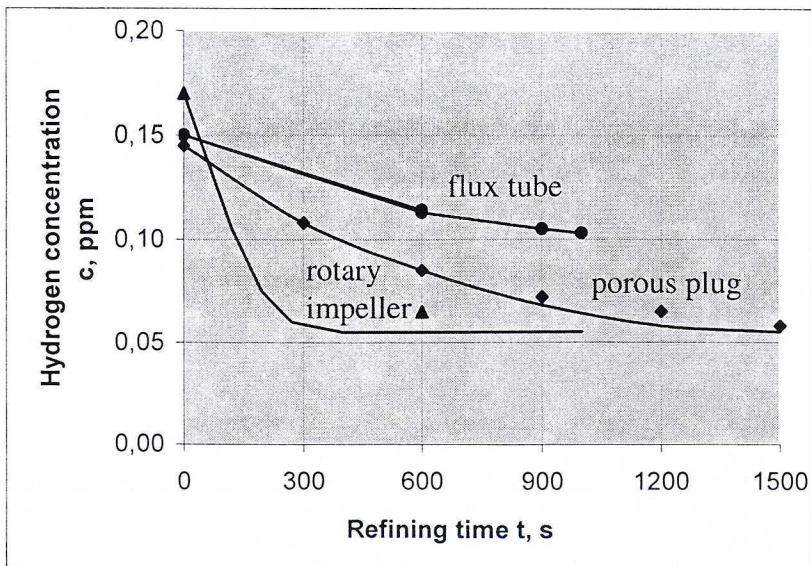

Fig. 1. Comparison of results obtained with three different degassing techniques of Al-Si-Mg alloy in a 200 kg furnace ($T = 1033$ K, $q = 6$ dm^3/min [2]

The results obtained with three methods, that is a flux tube, a porous plug and a rotary impeller are compared in Fig. 1. Three 200 kg batches of Al-Si-Mg alloy were degassed using the same flow rate of refining gas, and all conditions were maintained constant apart from the method of gas introduction. We can claim that the method of gas introduction to the liquid melt has a great influence on the time and course of the degassing process.

2. Mathematical model

2.1. The mechanism of the degassing process

The mechanism of the desorption process of gases soluble in liquid metals and the critical review and basic aspects of kinetics of gases desorption from liquid metals, especially from aluminium, were presented in the earlier paper [1].

For the system: hydrogen dissolved in liquid aluminium – purge gas, the studies were carried out by Pehlke and Bement [3] and Botor [4, 5]. In both cases it was found that the hydrogen degassing from liquid aluminium by purge gases has a diffusion character and is controlled by mass transport in the liquid metallic phase.

2.2. The review of available mathematical models

The short characteristics of the available mathematical models describing the aluminium refining process by purging gases was presented in [1]. The first model was created by Botor [4]. This model can not be used for the mathematical description of refining process in industrial conditions because it was created for interpreting the experimental data on a laboratory scale.

Dantzig, Clumpner and Tyler [6] assumed that there is no movement in liquid metallic phase. It is rather difficult to meet such conditions in most industrial reactors. This model can not be applied to process whit significant circulation of the melt by the refining gases, nor at high level of melt turbulence, which would substantially alter the effective diffusivity of hydrogen.

The most universal is the model presented by Sigworth and Engh [7]. Using this model we can draw some conclusions about the rate controlling stage of the process of hydrogen removal from liquid aluminium. We can do this by means of the dimensionless number Φ/c_t. This number represents the ratio of the ability of hydrogen to diffuse to bubbles during their ascent to the capacity of the purge gas to remove hydrogen:

$$\frac{\Psi}{c_t} = \frac{k \cdot \rho \cdot A \cdot p_{inert} \cdot K^2}{4 \cdot 100 \cdot \gamma^{`2}_{[H]Al} \cdot m_H \cdot \dot{G}} \cdot \frac{1}{c_t}, \tag{1}$$

where: $\dot{G}$ – molecular flow rate of inert gas, kmol/s,

Ψ – maximum hydrogen that can diffuse to bubbles, wt. %,

ρ – density of liquid aluminium, kg/m^3,

m$_H$ – molecular weight of hydrogen, g/mol,

p$_{inert}$ – pressure of inert gas, atm,

γ° $_{[H]Al}$ – hydrogen activity coefficient in aluminium,

K – equilibrium constant, %atm$^{-0.5}$,

A – interfacial contact area of bubbles in melt, m^2,

k – mass transfer coefficient, m/s,

c$_t$ – final hydrogen concentration after degassing, wt. %.

When $\Psi/c_t < 0.3$ [8] the diffusion of hydrogen in the metal is rate controlling; when $\Psi/c_t > 2$ [8] the thermodynamic equilibrium is reached.

The suggested mathematical description of the aluminium refining in the continuous reactor under the atmospheric pressure and the vacuum based on the equation (1) is presented below.

2.3. The mathematical model for the continuous reactor under the atmospheric pressure

The assumptions were made that: the hydrogen desorption from liquid aluminium is a diffusion process controlled by mass transfer of hydrogen in the liquid metallic phase; as well as the metal bath is well stirred so that the hydrogen concentration is essentially uniform. We assume also that the following equation:

$$p_{H_2} + p_{\text{inert}} = P, \tag{2}$$

where: p_{H_2} – partial pressure of hydrogen, atm,

P – total pressure in the gas bubble, atm,

is valid and the total pressure in the gas bubble is constant, $p_{H_2} << p_{\text{inert}}$ and so p_{inert} is constant and equals the atmospheric pressure. The gas bubble surface area is not a function of height in the bath and there is no mass exchange on the surface of the liquid metal. The amount of hydrogen removed from the aluminium equals the amount of hydrogen in the escaping bubbles. The entering stream of metal has a constant initial hydrogen content c_i. After some initial transient time we find that exit stream reaches a constant value of c_t. The equation of mass balance is expressed in the form:

$$\frac{\dot{M} \cdot (c_i - c_t)}{100 \cdot m_H} = 2\dot{G} \cdot \frac{p_{H_2}}{p_{atm}}, \tag{3}$$

where: $\dot{M}$ – flow rate of liquid aluminium in continuous reactor, kg/s.

In the case of diffusion control we find that:

$$\left(\frac{c_i}{c_t} - 1 \right) = \frac{k\rho A}{\dot{M}}. \tag{4}$$

The solution of the equation (3) in the kinetic range is the following relationship:

$$c_t = \frac{- B'' + \sqrt{(B'')^2 + 4B''c_i}}{2},$$

(5)

where:

$$B'' = \frac{K^2 \cdot p_{atm} \cdot \dot{M}}{200\, \gamma^{\,2}_{[H]Al} \cdot \dot{G} \cdot m_H},\ \%\ \text{mas.}$$

(5a)

2.4. The mathematical model for the continuous reactor under vacuum

A mass balance equation for the hydrogen leaving the section of the melt and entering inert gas phase for the atmospheric pressure can be written:

$$\Delta \left(\frac{p_{H_2}}{p_{\text{inert}}} \right) = \frac{k \cdot \rho \cdot \Delta A \cdot c}{100 \cdot m_H \cdot \dot{G}} \cdot \left(1 - \frac{K\sqrt{p_{H_2}}}{\gamma_{[H]Al} \cdot c} \right).$$

(6)

Most of the terms in equation (6) change with the height in the vacuum. The pressure decreases slightly as the bubble comes nearer to the surface, and the volume of gas bubble increases (Fig. 2). The mass transfer coefficient decreases slightly as the bubble grows and the bubble rise velocity increases.
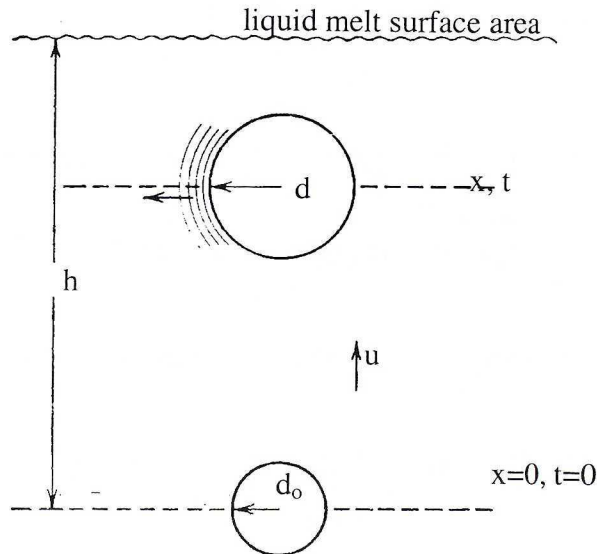

Fig. 2. Growth of the ascending bubble [9]

As for the case of diffusion control the solution of the equation (6) can be given in the form of:

$$\frac{p_{H_2}}{p_{\text{inert}}(h_o = h)} \cong [1 + a_p]^{12/7} - 1, \tag{7}$$

where: $a_p = \dfrac{k_o \cdot \rho \cdot A_o \cdot c}{200\, m_H \cdot \dot{G}} \cdot \dfrac{p_t^o}{\rho \cdot g \cdot h} \cong \dfrac{k_o \cdot \rho \cdot A_o \cdot c}{200\, m_H \cdot \dot{G}},$ \qquad (7a)

h_o – distance travelled by bubble from the bottom, m,
A_o – interfacial contact area of bubbles at bottom of melt, m²,
k_o – mass transfer coefficient of hydrogen at bottom of melt, m/s,
p_t^o – total pressure at bottom of melt, atm,
h – height of liquid aluminium, m.

Using a Maclaurin series in "a_p" the solution of the equation (7) can be written in the form of:

$$\frac{p_{H_2}}{p_{\text{inert}}} \cong \frac{12}{7} a_p + \frac{30}{49} a_p^{\,2} + \dots. \tag{8}$$

The second and higher terms may be neglected because "a_p" is less than 0,1.

To calculate the hydrogen concentration after some definite time for a continuous reactor we can use the equation (9), which describe also the degassing rate of the refining process:

$$\frac{c_i}{c_t} - 1 = \left[\frac{12}{7} \cdot \frac{k_o \cdot \rho \cdot A_o}{\dot{M}} \cdot \frac{p_t^o}{\rho \cdot g \cdot h} + \frac{k_1 \cdot \rho \cdot A_s}{\dot{M}} \right]. \tag{9}$$

where: k_1 – mass transfer coefficient at the melt surface, m/s,
A_s – melt surface area, m².

The equation (9) is valid, when $a_p \leq 0.1$ and dimensionless number Ψ/c_t, which can be written in the form of:

$$\Psi/c_t = \frac{k_o \cdot \rho \cdot A_o \cdot p_t^o \cdot K^2}{400\, \gamma_{[H]Al}^{\,2} \cdot m_H \cdot \dot{G}} \cdot \frac{1}{c_t} \cdot \frac{p_t^o}{\rho g h}, \tag{10}$$

is less than 0.2 (the diffusion control). These two conditions would be met in most industrial processes.

3. The selection of basic thermodynamic and kinetic parameters

The mathematical description of hydrogen degassing from liquid aluminium is possible if the thermodynamic and kinetic conditions of this process are defined. From the thermodynamic point of view the data of hydrogen solubility in liquid aluminium and its alloys are necessary. From the kinetic point a hydrogen degassing process is controlled by the mass transfer in the liquid aluminium and, accordingly, the very important problem is to estimate the mass transfer coefficient. The value of this coefficient is dependent on the hydrodynamic conditions of this process and transport features such as: the state of the interfacial surface, the gas bubble diameter and the bubble rise velocity. The critical review of the available literature [3–8] has shown that these parameters are not satisfactorily known. Many authors use different ways to calculate and determine these parameters and, accordingly, there is a necessity to select the basic thermodynamic and kinetic parameters of hydrogen desorption process.

3.1. The hydrogen solubility in liquid aluminium and its alloys

The hydrogen solubility in liquid aluminium is known from the experimental data. The values of this solubility vary to a certain degree from one investigator to another [10–18], no doubt because of the experimental difficulties. The selection of relationships describing the hydrogen solubility in liquid aluminium is essential to the mathematical description of refining process.

The analysis of the experimental data of hydrogen solubility in liquid aluminium let us select the most reliable values: [12, 13, 15] and [17]. The least square estimation of this values was carried out obtaining the following equation:

$$\log c = - \frac{2760 \pm 6.9}{T} + (2.813 \pm 0.0067) + 0.5 \log p_{H_2}, \qquad (11)$$

where: c – hydrogen solubility in aluminium, 1ppm = 10^{-4}% wt. = 1.12 cm³/100g Al,
  T – temperature, K.

The diatomic gases dissolving in melts follow the Sieverts' law. For pure aluminium the hydrogen solubility equals the value of equilibrium constant. The formula for this equilibrium constant as a function of temperature can be written in the form of:

$$\log K = - \frac{2760}{T} + 2.813 . \qquad (12)$$

The hydrogen solubility in aluminium alloys changes considerably depending on alloying elements. This solubility could be estimated by means of interaction parameters used for describing the activity in multicomponent alloys. For an Al-H-X system the

relationship between log $\gamma\grave{}_{[H]Al}$ and the concentration of alloying elements in wt. % can be described by the equation:

$$\log \gamma\grave{}_H = \sum_{Me=2}^{n} e_H^{Me} (\% Me) + \sum_{Me=2}^{n} r_H^{Me} (\% Me)^2 + \text{higher order terms}, \qquad (13)$$

where: e_H^{Me} – the first order interaction parameter,
r_H^{Me} – the second order interaction parameter,
Me – metal.

The interaction parameters for hydrogen solubility in liquid aluminium alloys as a function of melt temperature were given in Table 1 [19]. The linear expression for log $\gamma\grave{}_{[H]Al}$ in the equation (13) and the W a g n e r' s interaction parameters (Table1) are used for calculation of the hydrogen solubility in a multicomponent aluminium alloy.

TABLE 1

The first and second order interaction parameters for liquid Al-H-Me alloys as a function of temperature

Alloying elements, Me	Temperature, K				Reference number
	973	1023	1073	1123	
1	2	3	4	5	6
Cu (<32%) e_H^{Cu} r_H^{Cu}	0.0334 − 0.00065	0.0310 − 0.00058	0.0286 − 0.00052	0.0266 − 0.00046	[13]
Si (< 16%) e_H^{Si} r_H^{Si}	0.0193 − 0.00045	0.0189 − 0.00050	0.0182 − 0.00053	0.0181 − 0.00059	[13, 20]
Mg (< 6%) e_H^{Mg}	− 0.0660	− 0.0660	− 0.0660	− 0.0660	[21]
Zn (< 8%) e_H^{Zn}	0.0163	0.0171	(0.0138)	(0.0120)	[21, 22]
Li (< 3%) e_H^{Li}	− 0.2500	− 0.2500	− 0.2500	− 0.2500	[23, 24]
Fe (10%) e_H^{Fe}	0.0659	0.0505	0.0371	0.0246	[20]
Ti (4%) e_H^{Ti}	− 0.0205	− 0.0295	− 0.0375	− 0.0444	[20]
Zr (< 0.8%) e_H^{Zr}	–	− 0.8077	–	–	[18]
Ni e_H^{Ni}	0.0400	0.0400	0.0400	–	[10]
Mn e_H^{Mn}	–	–	0.0600	–	[10]
Sn e_H^{Sn}	–	–	0.0040	0.0040	[11]

3.2. The interfacial contact area

The rate of the degassing process is directly proportional to the interfacial contact area. If we know the gas bubble diameter and the bubble rise velocity, we can estimate the interfacial contact area from the following equation:

$$A = \frac{6qh}{ud},\tag{14}$$

where: d – gas bubble diameter, m,

u – bubble rise velocity, m/s,

q – flow rate of refining gas, m³/s.

For liquid metals, a direct experimental measurement of bubble rise velocity is impossible, contrary to water and organic liquids. However the good agreement (Fig. 3) of the velocity values calculated from Davies and Taylor's [25] equation:

$$u = 1.02 \sqrt{\frac{gd}{2}},\tag{15}$$

where: g – acceleration due to gravity, m/s²,

and these measured for water and CHBr · CHBr-CH₃OH solution whose density (2.37 g/cm³) is quite similar to the liquid aluminium density, let us use this equation for the calculation of the bubble rise velocity. It is very important to remember that the gas bubble diameter influences both: the area of mass exchange surface and the bubble rise velocity. The gas bubble diameter ranges from 0.005 m to 0.015 m. The gas bubbles with the increase of the flow rate of refining gas, can take various shapes, from a spherical one, through an oblate ellipsoid, to a spherical cup.
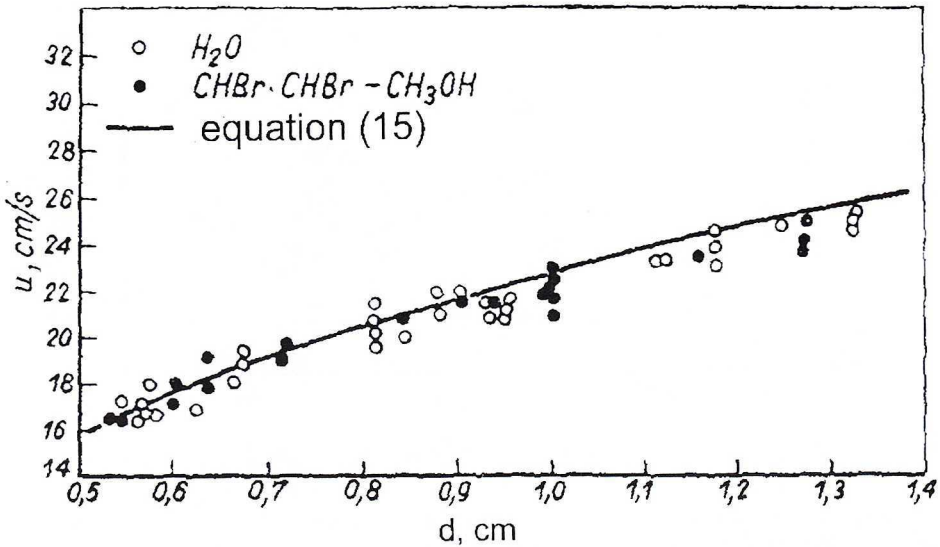

Fig. 3. The velocity of nitrogen bubble rise in water and CHBr·CHBr-CH₃OH solution. Full line calculated from equation (15) [4]

3.3. The mass transfer coefficient

The mass transfer coefficient can be theoretically estimated (the necessity of estimation the mass transfer coefficients in the gaseous and liquid phase), calculated from empirical correlations and experimentally determined (P e h l k e and B e m e n t [3], B o t o r [4]). The usability of the theoretical models of mass transfer (the boundary layer model, H i g b i e ' s penetration theory, the turbulent boundary layer) is considerably limited.

Basing on the B o t o r ' s [4, 5] experimental data, S i g w o r t h and E n g h [7] presented the following equation for the calculation of the mass transfer coefficient:

$$k = 0.0122e^{-24685.6/RT} (d_e/1.37)^{-\frac{1}{4}} \qquad (16)$$

where: R – gas constant, J/mol·K,

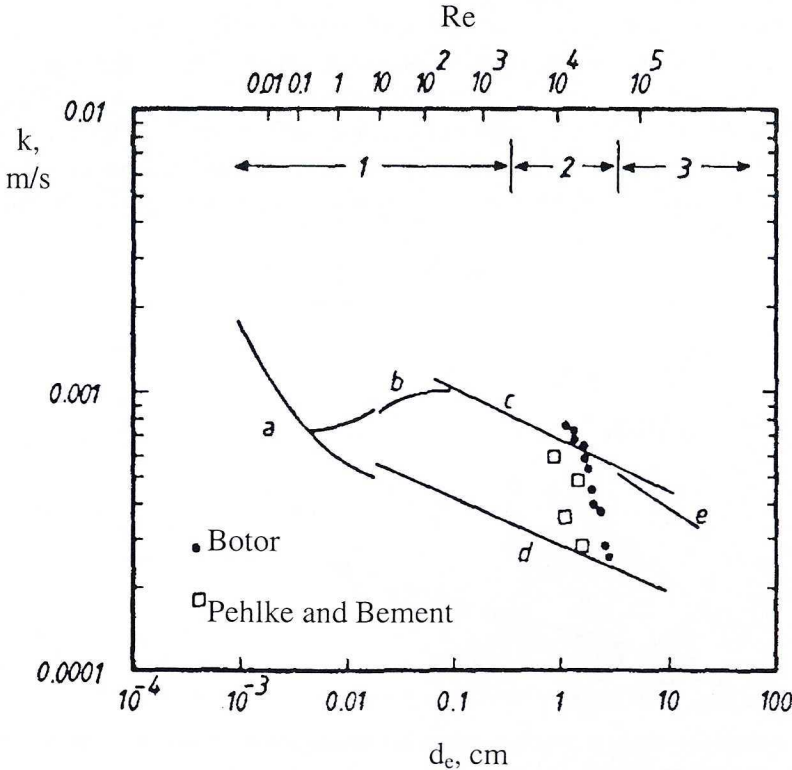d_e – equivalent gas bubble diameter, m.

Fig. 4. Predicted and observed [4, 5] mass transfer coefficient for the removal of hydrogen to inert gas bubbles in aluminium at 1000 K. (regimes 1, 2 i 3 correspond to spherical, ellipsoid and spherical cup bubbles; a – mass transfer for viscous flow, b – mass transfer for turbulent flow to a circulating bubble in the transition region, c – mass transfer to a circulating bubble in potential flow, d – mass transfer to a rigid bubble in potential flow, e – mass transfer to the front and rear face of a spherical cup bubble

This equation takes into account the influence of temperature and the change of the equivalent gas bubble diameter. The change of the mass transfer coefficient as a function of the equivalent gas bubble diameter was presented in Fig. 4. Here, the theoretical results [26] calculated for various shapes and for various flow rates of purge gas and the experimental data measured by B o t o r [4,5] and P e h l k e and B e m e n t [3] were compared. P e h l k e and B e m e n t ' s data were recalculated by S i g w o r t h and E n g h [7] using the equation (8). For the aluminium refining process the gas bubble diameter ranges from 0.005 m to 0.015 m. Within this range the values of the mass transfer coefficient estimated from B o t o r ' s experimental data and P e h l k e and B e m e n t ' s recalculated data seem to be the most reliable.

4. The verification of results

4.1. The continuous reactor under the atmospheric pressure

The results of the AK-64 alloy refining using nitrogen as a purge gas in the experimental continuous reactor were presented in [27]. The experiments were carried out under the industrial conditions. The scheme of refining reactor was presented in [27]. The refining reactor consisted of three chambers. There was the counter-current flow of gas bubbles generated by two porous plugs in the first one. The vertical flow of metal to the direction of gas flow was observed in the second chamber, in which four porous plugs were installed. The third chamber was used as a decanter, and metal leaving this chamber was directed to the casting machine. The capacity of reactor was about 1500 kg of liquid aluminium, and the rate of production about 5000 kg Al/h.

Chemical analysis of the AK-64 was the following: 4% Cu, 1.20% Fe, 0.50% Mn, 0.50% Mg, 0.20% Zn, 6% Si, 0.50% Ni, 0.15% Ti, 0.10% Sn, 0.30% Pb. The parameters of refining process were the following:
   a) temperature: 993 K – 1030 K,
   b) flow rate of refining gas: from 23.2 dm^3/min to 7.7 dm^3/min,
   c) as a purge gas nitrogen containing at least 99.8% N$_2$ was used,
   d) height of liquid aluminium – 0.65 m,
   e) 12 500 kg of AK-64 alloy was refined.

The hydrogen concentration in AK-64 alloy was determined using Dardel's method (the initial bubble test). The sample was taken from the tapping spout that connected the induction furnace with the refining reactor (c_i), and from the tapping spout connected the refining reactor with the casting machine (c_t). The results of refining were presented in Table 2 (column ''2'' and ''3''). In Table 3 the basic parameters of refining and necessary data for calculation were juxtaposed.

The results of hydrogen concentration after refining process in continuous reactor under the atmospheric pressure

Melt	c_i, cm³/100g	c_t, cm³/100g	Ψ/c_t	c_t (cal), cm³/100g	Ψ/c_t	$\dot{G}$, kmol/s	T, K
1	2	3	4	5	6	7	8
I	0.459	0.175		$d_e = 0.010$ m			
			0.025	0.263	0.017	$1.72 \cdot 10^{-5}$	993
				0.291	0.015	$1.33 \cdot 10^{-5}$	
				0.313	0.014	$1.08 \cdot 10^{-5}$	
				0.368	0.012	$0.57 \cdot 10^{-5}$	
			0.049	0.251	0.034	$1.72 \cdot 10^{-5}$	1030
				0.280	0.031	$1.33 \cdot 10^{-5}$	
				0.302	0.028	$1.08 \cdot 10^{-5}$	
				0.359	0.024	$0.57 \cdot 10^{-5}$	
				$d_e = 0.005$ m			
			0.084	0.131	0.112	$1.72 \cdot 10^{-5}$	993
				0.156	0.094	$1.33 \cdot 10^{-5}$	
				0.178	0.082	$1.08 \cdot 10^{-5}$	
				0.251	0.058	$0.57 \cdot 10^{-5}$	
			0.165	0.121	0.238	$1.72 \cdot 10^{-5}$	1030
				0.146	0.197	$1.33 \cdot 10^{-5}$	
				0.167	0.173	$1.08 \cdot 10^{-5}$	
				0.239	0.120	$0.57 \cdot 10^{-5}$	
II	0.417	0.199		$d_e = 0.010$ m			
			0.022	0.239	0.018	$1.72 \cdot 10^{-5}$	993
				0.265	0.016	$1.33 \cdot 10^{-5}$	
				0.284	0.015	$1.08 \cdot 10^{-5}$	
				0.334	0.013	$0.57 \cdot 10^{-5}$	
			0.043	0.228	0.038	$1.72 \cdot 10^{-5}$	1030
				0.254	0.037	$1.33 \cdot 10^{-5}$	
				0.274	0.031	$1.08 \cdot 10^{-5}$	
				0.327	0.026	$0.57 \cdot 10^{-5}$	

1	2	3	4	5	6	7	8
II	0.417	0.199			$d_e = 0.005$ m		
			0.074	0.119	0.124	$1.72 \cdot 10^{-5}$	993
				0.142	0.103	$1.33 \cdot 10^{-5}$	
				0.162	0.091	$1.08 \cdot 10^{-5}$	
				0.228	0.064	$0.57 \cdot 10^{-5}$	
			0.146	0.110	0.262	$1.72 \cdot 10^{-5}$	1030
				0.132	0.217	$1.33 \cdot 10^{-5}$	
				0.152	0.190	$1.08 \cdot 10^{-5}$	
				0.217	0.132	$0.57 \cdot 10^{-5}$	
III	0.370	0.160			$d_e = 0.010$ m		
			0.027	0.212	0.021	$1.72 \cdot 10^{-5}$	993
				0.235	0.019	$1.33 \cdot 10^{-5}$	
				0.252	0.017	$1.08 \cdot 10^{-5}$	
				0.296	0.015	$0.57 \cdot 10^{-5}$	
			0.054	0.202	0.042	$1.72 \cdot 10^{-5}$	1030
				0.226	0.038	$1.33 \cdot 10^{-5}$	
				0.243	0.035	$1.08 \cdot 10^{-5}$	
				0.290	0.030	$0.57 \cdot 10^{-5}$	
					$d_e = 0.005$ m		
			0.092	0.105	0.139	$1.72 \cdot 10^{-5}$	993
				0.126	0.116	$1.33 \cdot 10^{-5}$	
				0.144	0.102	$1.08 \cdot 10^{-5}$	
				0.202	0.072	$0.57 \cdot 10^{-5}$	
			0.181	0.098	0.295	$1.72 \cdot 10^{-5}$	1030
				0.118	0.245	$1.33 \cdot 10^{-5}$	
				0.135	0.214	$1.08 \cdot 10^{-5}$	
				0.193	0.149	$0.57 \cdot 10^{-5}$	
IV	0.483	0.198			$d_e = 0.010$ m		
			0.022	0.276	0.016	$1.72 \cdot 10^{-5}$	993
				0.306	0.014	$1.33 \cdot 10^{-5}$	
				0.329	0.013	$1.08 \cdot 10^{-5}$	
				0.387	0.011	$0.57 \cdot 10^{-5}$	

1	2	3	4	5	6	7	8
IV	0.483	0.198	0.043	0.264	0.033	$1.72 \cdot 10^{-5}$	1030
				0.295	0.029	$1.33 \cdot 10^{-5}$	
				0.318	0.027	$1.08 \cdot 10^{-5}$	
				0.379	0.023	$0.57 \cdot 10^{-5}$	
			$d_e = 0.005$ m				
			0.074	0.138	0.107	$1.72 \cdot 10^{-5}$	993
				0.164	0.089	$1.33 \cdot 10^{-5}$	
				0.187	0.078	$1.08 \cdot 10^{-5}$	
				0.264	0.055	$0.57 \cdot 10^{-5}$	
			0.146	0.128	0.226	$1.72 \cdot 10^{-5}$	1030
				0.153	0.188	$1.33 \cdot 10^{-5}$	
				0.176	0.164	$1.08 \cdot 10^{-5}$	
				0.264	0.114	$0.57 \cdot 10^{-5}$	
V	0.390	0.103	$d_e = 0.010$ m				
			0.043	0.223	0.020	$1.72 \cdot 10^{-5}$	993
				0.247	0.018	$1.33 \cdot 10^{-5}$	
				0.266	0.016	$1.08 \cdot 10^{-5}$	
				0.312	0.014	$0.57 \cdot 10^{-5}$	
			0.084	0.213	0.040	$1.72 \cdot 10^{-5}$	1030
				0.238	0.036	$1.33 \cdot 10^{-5}$	
				0.257	0.033	$1.08 \cdot 10^{-5}$	
				0.306	0.028	$0.57 \cdot 10^{-5}$	
			$d_e = 0.005$ m				
			0.143	0.111	0.132	$1.72 \cdot 10^{-5}$	993
				0.133	0.110	$1.33 \cdot 10^{-5}$	
				0.151	0.097	$1.08 \cdot 10^{-5}$	
				0.213	0.069	$0.57 \cdot 10^{-5}$	
			0.280	0.103	0.280	$1.72 \cdot 10^{-5}$	1030
				0.124	0.232	$1.33 \cdot 10^{-5}$	
				0.142	0.203	$1.08 \cdot 10^{-5}$	
				0.203	0.141	$0.57 \cdot 10^{-5}$	

TABLE 3

The basic parameters of AK-64 alloy refining and the necessary data for calculation

Temperature T, K		993	1003
Activity coefficient $\gamma_{[H]Al}$		1.89	1.78
Equilibrium constant K, %atm$^{-0.5}$		$9.65 \cdot 10^{-5}$	$1.21 \cdot 10^{-4}$
Alloy density ρ, kg/m^3		2352.2	2342.4
Mass transfer coefficient	$d = 0.010$ m	$6.64 \cdot 10^{-4}$	$7.39 \cdot 10^{-4}$
k, m/s	$d = 0.005$ m	$7.89 \cdot 10^{-4}$	$8.79 \cdot 10^{-4}$
Bubble diameter d, m	Flow rate of gas q, dm^3/min	Interfacial contact area of bubbles in melt A, m^2	
0.005	23.2	1.88	
	17.8	1.45	
	14.5	1.18	
	7.7	0.62	
0.010	23.2	0.67	
	17.8	0.51	
	14.5	0.42	
	7.7	0.22	

Fig. 5. The final hydrogen concentration as a function of temperature and the gas bubble diameter when $q = 23.2$ dm^3/min

336

The calculations were carried out for four following values of molecular flow rate of refining gas: $1.72 \cdot 10^{-5}$ kmol/s; $1.33 \cdot 10^{-5}$ kmol/s; $1.08 \cdot 10^{-5}$ kmol/s, $0.57 \cdot 10^{-5}$ kmol/s and two temperatures: 993 K and 1030 K. The results of calculations were presented in Table 2. The equivalent gas bubble diameter was assumed to be 0.010 m and 0.005 m. The values of Φ/c_t (column "4" – for c_t from experimental data, column "6" – for c_t(cal) calculated) were calculated from equation (1), the values of c_t(cal) – column "5" – from equation (4).

The final hydrogen concentration as a function of temperature and equivalent gas bubble diameter when the flow rate of gas equals 23.2 dm³/min was presented in Fig. 5. The final hydrogen concentration as a function of the flow rate of refining gas when $T = 993$ K and $d_e = 0.005$ m was shown in Fig. 6.

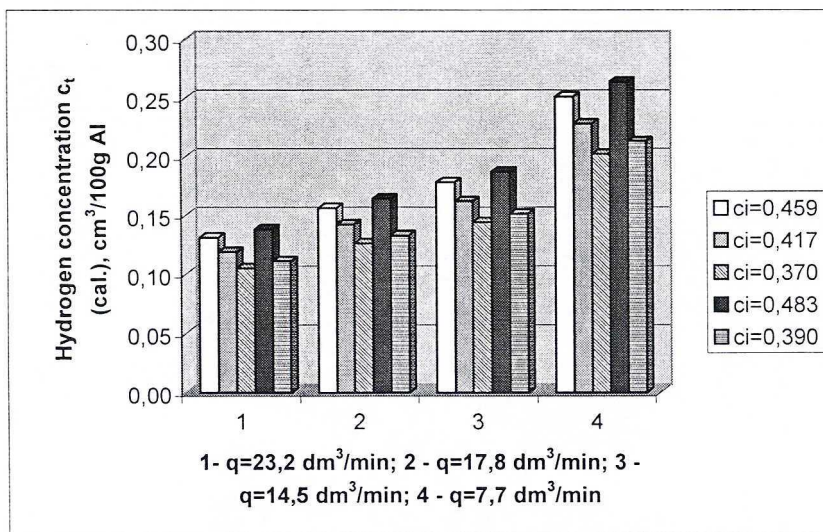Fig. 6. The final hydrogen concentration as a function of flow rate at $T = 993$ K and $d_e = 0.005$ m

4.2. The continuous reactor under vacuum

Using the results of AK-64 alloy refining carried out in the continuous reactor under the atmospheric pressure the calculations for refining this alloy in the vacuum were done. The height of liquid aluminium is 0.65 m, so the total pressure at the bottom of the melt will be $p_t^o = 0.15$ atm. The calculations were done assuming that the initial gas bubble diameter is 0.006 m at $T = 993$ K and $q = 23.2$ dm³/min. The values of: the contact area of bubbles at bottom of melt A_o, the mass transfer coefficient at bottom of melt k_o and the bubble rise velocity at bottom of melt u_o were estimated from equations (14), (15) and (16). The value of "d" in these equations was replaced with d_o – initial gas bubble diameter at the bottom of melt. Equation (9) was used for calculating the hydrogen concentration after refining.

The results of calculations for continuous reactor under vacuum in comparison with the calculations under the atmospheric pressure were presented in Table 4.

TABLE 4

The results calculations for AK-64 alloy after refining in continuous reactor under vacuum

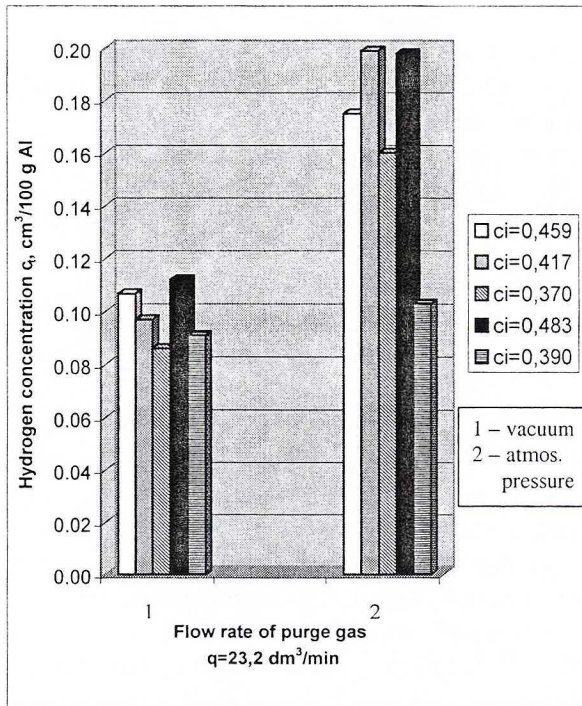| c_i cm³/100g Al	c_t cm³/100g Al	c_t from (4), cm³/100g Al atm. pressure	Ψ/c_t – from (1), atm. pressure	Ψ/c_t – from (10), vacuum	$\dfrac{p_{H_2}}{p_{atm}}$	q cal. vacuum, dm³/min	c_t, q from col. 9, vacuum, cm³/100g Al	c_t, $q = 23.2$ dm³/min, vacuum, cm³/100g Al
1	2	3	4	5	6	7	8	10
0.459	0.175	0.162	0.061	0.009	0.020	11.98	0.168	0.107
0.417	0.199	0.147	0.054	0.008	0.022	8.08	0.190	0.097
0.370	0.160	0.131	0.067	0.010	0.018	9.68	0.153	0.086
0.483	0.198	0.171	0.054	0.008	0.022	10.62	0.189	0.112
0.390	0.103	0.138	0.104	0.015	0.012	20.57	0.101	0.091

Fig. 7. The final hydrogen concentration calculated for the atmospheric pressure (2) and for a vacuum (1) at the same flow rate of refining gas (23.2 dm³/min)

In column "1" and "2" the values of hydrogen concentration in AK-64 alloy before and after refining under the atmospheric pressure were presented, respectively. The results of hydrogen concentration after refining under the atmospheric pressure calculated from equation (4), when d = 0.006 m, were juxtaposed in column "3".

The values of the dimensionless number Ψ/c_t calculated from equation (1) for the atmospheric pressure and from equation (10) for a vacuum were presented in column "4" and "5" respectively. When we put the value of ratio p_{H_2}/p_{inert} (column "6") – calculated from equation (8) – in the equation (3), we can calculate the flow rate of refining gas which is adequate to the known initial hydrogen concentration and desirable final hydrogen concentration. The calculated values of flow rate of purge gas in a vacuum were presented in column "7". The values of hydrogen concentration calculated from equation (9) when the flow rate of purge gas was calculated from equation (3) and equal 23.2 dm³/min were presented in column "8" and "9" respectively. The values of final hydrogen concentration under the atmospheric pressure and under vacuum at the same flow rate of refining gas (23.2 dm³/min) were presented in Fig. 7.

5. Discussion and conclusion

This work consists of three parts:
- Modelling calculations of hydrogen removal process from liquid aluminium using the dimensionless number Ψ/c_t introduced by Sigworth and Engh [7] and based on the rate of chemical reaction and mass transport.
- Selection of the kinetic and thermodynamic parameters which are essential to the mathematical description of the aluminium refining process.
- The verification of this mathematical model – the comparison of the experimental data (AK-64 alloy) with calculated values.

The hydrogen solubility in liquid aluminium and its alloys, the area of mass exchange surface and mass transfer coefficient are the most important kinetic and thermodynamic parameters whose knowledge is essential to the mathematical calculations.

The analysis of experimental data of hydrogen solubility in liquid pure aluminium led us to select the most reliable values. For the aluminium alloys this solubility was estimated, taking into account the influence of the alloying elements.

Because there is lack of available experimental data the calculations of the equilibrium constant in Sieverts' equation were done taking into account the activity coefficient. This coefficient was estimated from Wagner's interaction parameters (Table 1). The choice of Wagner's parameters was made basing on the selection of the available literature data [10, 11, 13, 18–24]. The source data in this range are not so extensive, especially concerning the second order interaction parameters [13, 20]. The temperature dependences are generally lacking.

The interfacial contact area was estimated from equation (6). Although the changeable hydrodynamic conditions can influence the value of the interfacial contact area in the aluminium degassing process, there is no better method to determine this area.

We know from earlier experimental research [3–5] that the hydrogen degassing process from liquid aluminium has a diffusion character. Because of this, the knowledge of the mass transfer coefficient is essential. It was found that the Botor's [4, 5] and Pehlke and

Bement's [3] experimental data which were presented by Sigworth and Engh [7] in equation (16) seem most reliable.

Equation (16) has a general character. If we know the value of activation energy of diffusion we can estimate the mass transfer coefficient in liquid phase for other systems metal – gas, assuming that the mass transport in liquid phase is rate controlling. The values of the diffusion coefficient of hydrogen and activation energy of diffusion for iron, copper and nickel were presented in Table 5.

TABLE 5

The diffusion coefficient of hydrogen and activation energy of diffusion for liquid metals

	Reference number	Temperature T, K	Diffusion coefficient D, cm^2/s	Self-diffusion coefficient A_1, cm^2/s	Activity energy E_D, kJ/mol
1	2	3	4	5	6
Fe – H	[28, 29]	1873	$132 \cdot 10^{-5}$	$3.20 \cdot 10^{-3}$	13.80
Cu – H	[28, 30]	1473	$(126 \div 525) \cdot 10^{-5}$	$10.90 \cdot 10^{-3}$	8.99
Ni – H	[28]	1773	$(66 \div 320) \cdot 10^{-5}$	$7.50 \cdot 10^{-3}$	35.60

The analysis of aluminium alloys refining process was carried out basing on the results of calculations and experimental data. The value of dimensionless number Ψ/c_t is the criteria of applicability of the presented model. The calculated values of Ψ/c_t for the continuous reactor under the atmospheric pressure are less than 0.3 (Table 2). According to this, the process of hydrogen desorption is controlled by mass transfer in the liquid aluminium phase.

When the refining process for AK-64 alloy is conducted under vacuum and the total pressure at the bottom of melt is equal to 0.15 atm, we can say that the values of Ψ/c_t are less than 0.2 what means that the process has diffusion character. It can be noticed that the values of Ψ/c_t in vacuum are less than values of this number for the process under the atmospheric pressure (Ψ/c_t in vacuum = 15% Ψ/c_t in atmospheric pressure).

The agreement of the experimental data with the calculated results (Table 2) and the obtained values of the gas bubble diameter (from 0.005 m to 0.010 m) confirm the reliability of this model and selected parameters. The hydrogen removal process from liquid aluminium and its alloys is well described by the presented mathematical model.

The calculations of the final hydrogen concentration were carried out for different flow rates of purge gas. The results have shown that the higher values of flow rate of refining gas cause the better degassing of the metal (Fig. 6). It is very important to remember that the gas bubbles change their shapes (from a spherical one, through an oblate ellipsoid, a spherical cap to the wobbling one) with the increase of the flow rate of refining gas. We should also take into consideration the fact that too high flow rate of refining gas can cause the undesirable catenary flow of refining gas.

There were also calculations presented for the refining reactor under vacuum. The analysis of the refining process under vacuum without gas purging was presented in Szweycer's work [31]. There are neither works nor results of studies concerning degassing by gas purging in vacuum. This fact causes that our mathematical simulation concerning vacuum can not be verified. The presented calculations have shown that when we used vacuum the flow rate of refining gas could be reduced even three times (Table 4). Although the flow rate of gas under vacuum is the same as under the atmospheric pressure, the better results of the hydrogen degassing could be obtained. If the process has diffusion character the approximate values of final hydrogen concentration could be estimated from equation (9).

The presented model for degassing by gas purging in vacuum seems to be reliable but the obtained results need to be compared with the experimental data.

REFERENCES

[1] M. Saternus, J. Botor, Rudy Metale 48(4), 154–160 (2003).

[2] T. A. Engh, T. Pedersen, Light Metals TMS, 1329–1344 (1984).

[3] R. D. Pehlke, A. I. Bement, A. Trans. AIME **224**, 1237–1242 (1962).

[4] J. Botor, Prace IMN Dodatek **7(1)**, 3–40 (1978).

[5] J. Botor, Aluminium **56**, 519–522 (1980).

[6] J. A. Dantzig, J. A. Clumpner, D. E. Tyler, Metall. Trans. B **11B**, 433–438 (1980).

[7] G. K. Sigworth, T. A. Engh, Metall. Trans. B **13B**, 447–460 (1982).

[8] T. A. Engh, Principles of Metal Refining, Oxford University Press, Oxford, 171–217 (1992).

[9] J. Szekely, N. J. Themelis, Rate Phenomena in Process Metallurgy, Wiley, New York, 695 (1971).

[10] W. Baukloh, F. Oesterlen, Z. Metallkd. **30**, 386–389 (1938).

[11] W. Baukloh, M. Redjali, Metallwirtschaft **21**, 683–688 (1942).

[12] C. E. Ransley, H. Neufeld, J. Inst. Metals **74**, 599–620 (1948).

[13] W. R. Opie, N. J. Grant, Trans. AIME **188**, 1237–1241 (1950).

[14] V. W. Eichenauer, K. Hattenbach, A. P. Darmstadt, Z. Metallkd. **52**, 682–684 (1961).

[15] D. E. J. Talbot, P. N. Anyalebechi, Mater. Sci. Technol. **4**, 1–4 (1988).

[16] A. San-Martin, F. D. Manchester, J. Phase Equilibria **13**, 17–21 (1992).

[17] H. Liu, M. Bouchard, L. Zhang, J. of Mat. Sc. **30**, 4309–4315 (1995).

[18] P. N. Anyalebechi, Light Metals 1998, San Antonio 827–842, (1998).

[19] M. Saternus, Ph.D. Thesis, Politechnika Śląska, Katowice 17, (2002).

[20] H. Shahani, Ph.D. Thesis, The Royal Institute of Technology, Stockholm, Sweden, (1984).

[21] A. A. Grigoreva, V. A. Danilkin, Tsvetnye Metally **1**, 90 (1984).

[22] D. Stephenson, Ph.D. Thesis, Brunel University, Middlesex, England (1978).

[23] P. N. Anyalebechi, D. E. J. Talbot, D. A. Granger, Metall. Trans. B **19B**, 227–232 (1988).

[24] M. Sargent, Ph.D. Thesis, Brunel University, Middlesex, England (1989).

[25] R. M. Davies, G. I. Taylor, Proc. Roy. Soc. **A 200**, 375 (1950).

[26] R. Clift, J. R. Grace, M. E. Weber, Bubbles, Drops and Particles, Academic Press, New York 27, 36, 48, 123, 135, 136, 214 (1978).

[27] J. Botor, Z. Pasich, P. Zgorzalewicz, S. Banaś, W. Zamarski, Rudy Metale **22(8)**, 392–398 (1977).

[28] F. D. Richardson, Physical Chemistry of Metals in Metallurgy **2**, 477–487 (1974).

[29] E. T. Turkdogan, Physical Chemistry of Oxygen Steelmaking Thermochemistry and Thermodynamics, United States Steel Corpn, (1970).

[30] E. M. Sacris, N. A. D. Parlee, Metall. Trans. **1**, 3377 (1970).

[31] M. Szweycer, Politechnika Poznańska — Rozprawy nr 102, 3—88 (1979).